The Microwave Spectrum of Methyl Selenocyanate (CH_3SeCN)

B. M. Landsberg

Physikalisch-Chemisches Institut der Universität Gießen *

Z. Naturforsch. **33a**, 1333–1340 (1978); received April 8, 1978

The microwave spectrum of methyl selenocyanate has been observed for the isotopic species $^{12}CH_3{}^{80}Se^{12}C^{14}N$, $^{12}CH_3{}^{78}Se^{12}C^{14}N$, $^{12}CH_3{}^{77}Se^{12}C^{14}N$, $^{12}CH_3{}^{76}Se^{12}C^{14}N$, $^{12}CH_3{}^{82}Se^{12}C^{14}N$, $^{13}CH_3{}^{80}Se^{12}C^{14}N$ and $^{13}CH_3{}^{78}Se^{12}C^{14}N$.

For the main isotopic species, a full centrifugal distortion analysis is reported and internal rotation splittings have been analysed for the ground and first excited torsional states, and also for the $v_{10} = 1$ and $v_{10} = 2$ excited vibrational states. A structure based on a mixture of r_s and r_0 arguments is reported, and also the principal components of the dipole moments.

I. Introduction

Although methyl selenocyanate has formerly been prepared [1, 3] its infra-red and Raman spectra characterised [1, 2] and its liquid phase dipole-moment measured [3], neither structural data nor microwave measurements have yet been reported.

The microwave spectrum between 8 and 40 GHz was measured, and the strongest transitions in the spectrum are a-type R-branch lines of a somewhat asymmetric rotor ($\varkappa \sim -0.77$). As the selenium atom has five important isotopes and as methyl-selenocyanate has internal rotation of the methyl group and a C–Se–C bending vibration [1, 2] of 168 cm^{-1} the spectrum of each rotational transition contains many lines. A scan of the microwave spectrum of methyl selenocyanate between 18.0 and 26.5 GHz is shown in Figure 1.

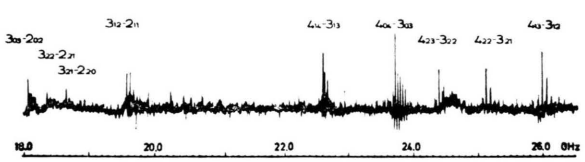

Fig. 1. Fast scan of the spectrum of CH_3SeCN between 18.0 and 26.5 GHz. Note the structure of each vibrational transition due to the isotopes of selenium and the low-lying vibrational states.

The rotational constants, structure, dipole-moment components and effective internal rotation barrier heights in the $v_{10} = 0$, 1 and 2 vibrationally excited states are reported, where v_{10} represents the lowest in-plane bending mode consisting mainly of the C–Se–C bending vibration. A strong dependence of the effective barrier height with increasing excitation of v_{10} has been observed, and the effect of this on the spectrum is illustrated in Figure 2.

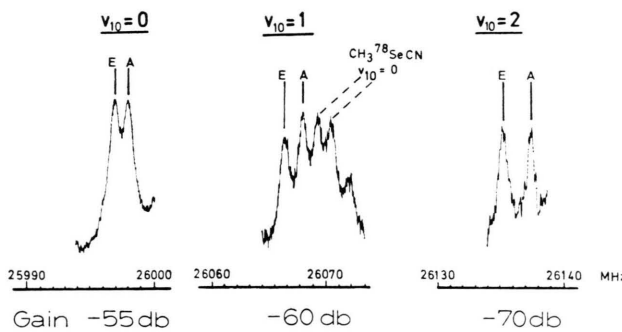

Fig. 2. The $4_{13} \leftarrow 3_{12}$ transition of CH_3SeCN in the $v_{10} = 0$, 1 and 2 states. The gain setting is a voltage db scale — i.e. every — 20 db increases the scale sensitivity by a factor of 10. The increase of internal rotation splitting with v_{10} is clearly shown.

II. Experimental Procedures

In the small scale preparation of the molecule, commercially available KSeCN was used, and converted to the silver salt by metathesis with aqueous silver nitrate. The precipitate was washed, dried and ground. The resultant powder was pumped under vacuum until thoroughly dry, and left to stand with methyl iodide for about six hours at room temperature. The volatile products were collected and vacuum distilled. $^{13}CH_3SeCN$ was prepared as above using ^{13}C enriched methyl iodide. The microwave spectra were recorded using a commercial Hewlett-Packard model 8460A MRR spectrometer. All spectra were taken at room temperature because it was not possible to cool the cell sufficiently due to the low vapour pressure of the molecule.

* Physikalisch-Chemisches Institut der Universität Gießen, Heinrich-Buff-Ring 58, D-6300 Gießen.

Reprint requests to Dr. B. M. Landsberg, University of Cambridge, Department of Physics, Cavendish Laboratory, Madingley Road, Cambridge CB 3 0HE, England.

Table 1. The observed and calculated rotational transition frequencies (in MHz) for the symmetry species A of $^{12}CH_3{}^{80}Se^{12}C^{14}N$ in the ground vibrational state.

$J'_{K_a'K_c'}$	$J''_{K_a''K_c''}$	Observed	Calc.[a]	Obs.− Calc.	$\nu_A - \nu_E$
7_{07}	6_{06}	39707.53[b]	39707.53	0.00	—
7_{17}	6_{16}	39057.15[b]	39057.19	−0.04	—
6_{24}	5_{23}	38529.73	38529.73	−0.00	1.79
6_{15}	5_{14}	38510.31	38510.31	0.00	1.41
6_{33}	5_{32}	37233.83	37233.78	0.05	—[c]
6_{34}	5_{33}	37000.49[b]	37000.50	−0.01	—
6_{25}	5_{24}	36347.85	36347.86	−0.01	0.76
6_{06}	5_{05}	34501.99[b]	34501.97	0.02	—
6_{16}	5_{15}	33632.41[b]	33632.37	0.04	—
5_{14}	4_{13}	32323.52	32323.54	−0.02	1.24
5_{23}	4_{22}	31778.97	31778.94	0.03	1.46
5_{24}	4_{23}	30405.63	30405.58	0.05	0.83
5_{05}	4_{04}	29201.14[b]	29201.15	−0.01	—
5_{15}	4_{14}	28153.29[b]	28153.30	−0.01	—
4_{13}	3_{12}	25997.98	25997.99	−0.01	1.09
4_{04}	3_{03}	23729.49[b]	23729.57	−0.08	—
4_{14}	3_{13}	22615.99[b]	22616.01	−0.02	—
3_{12}	2_{11}	19573.61	19573.54	0.07	0.93
3_{03}	2_{02}	18043.46[b]	18043.46	0.00	—
3_{13}	2_{12}	17021.95[b]	17021.95	−0.00	—
7_{16}	7_{17}	22993.84	22993.90	−0.06	—[c]
8_{17}	8_{18}	28850.89	28850.85	0.04	5.98
9_{18}	9_{19}	34904.31	34904.30	−0.01	6.82
10_{28}	10_{29}	22086.55	22086.54	−0.01	6.68
11_{29}	$11_{2\,10}$	28251.00	28250.98	0.02	—[c]
$12_{2,10}$	$12_{2,11}$	34838.81	34838.80	0.01	—[c]
$13_{3,10}$	$13_{3,11}$	18936.22	18936.15	0.07	7.98
$14_{3,11}$	$14_{3\,12}$	25076.07	25076.10	−0.03	9.70
$16_{3,13}$	$16_{3,14}$	39198.79	39198.79	0.00	—[c]
$17_{4,13}$	$17_{4,14}$	20262.63	20262.61	0.03	—[c]
$18_{4,14}$	$18_{4,15}$	26854.25	26854.27	−0.02	12.74
$19_{4,15}$	$19_{4,16}$	34231.04	34231.08	−0.04	14.79
$21_{5,16}$	$21_{5,17}$	20747.05	20747.05	−0.00	14.10
$22_{5,17}$	$22_{5,18}$	27650.24	27650.25	−0.01	15.67
$23_{5,18}$	$23_{5,19}$	35468.75	35468.77	−0.02	18.16
$25_{6,19}$	$25_{6,20}$	20576.47	20576.44	0.03	14.96
$26_{6,20}$	$26_{6,21}$	27646.38	27646.39	−0.01	18.16
$27_{6,21}$	$27_{6,22}$	35774.26	35774.29	−0.03	21.15
$29_{7,22}$	$29_{7,23}$	19907.97	19907.99	−0.02	16.30
$30_{7,23}$	$30_{7,24}$	27001.97	27001.97	−0.00	20.06
$31_{7,24}$	$31_{7,25}$	35297.76	35297.75	0.02	23.61
$33_{8,25}$	$33_{8,26}$	18877.44	18877.42	0.02	17.11
$34_{8,26}$	$34_{8,27}$	25861.46	25861.44	0.02	21.24
$35_{8,27}$	$35_{8,28}$	34180.80	34180.78	0.02	25.33
$38_{9,29}$	$38_{9,30}$	24356.35	24356.32	0.03	21.75
$39_{9,30}$	$39_{9,31}$	32559.03	32559.00	0.03	26.19
$42_{10,32}$	$42_{10,43}$	22604.47	22604.53	−0.06	21.45

[a] Calculated frequencies were obtained from Eq. (1) using the following least-squares adjusted spectroscopic constants (in MHz):

A	= 10143.867(31)	D_{JK}	= 0.01379(17)
B	= 3483.6892(24)	D_K	= 0.223(16)
C	= 2631.6454(24)	δ_J	= 0.0004026(47)
D_J	= 0.001101(34)	δ_K	= 0.0108(24)

[b] Internal rotation splitting unresolved. Frequencies corrected by half the calculated splitting using the ground state internal rotation parameters (Table 16).

[c] E species transition blended with other transitions.

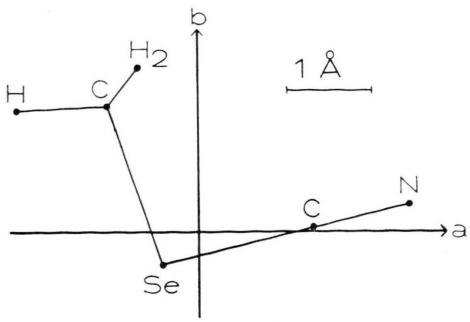

Fig. 3. The structure of the molecule CH_3SeCN projected on the a, b plane of the principal axis system. Angular position of methyl top is assumed.

The species $^{12}CH_3{}^{80}Se^{12}C^{14}N$ will throughout the paper be referred to as the "main" isotopic species, and it was for this species that not only the a-type R-branches but also the a-type Q-branches (up to $J = 42$, $K_a = 10$) were measured (Table 1). Unfortunately, neither b-type nor $\Delta K_a = 2$ transitions were observed. In principle every transition appears as a doublet due to internal rotation, but in some cases, these splittings were not resolved. In these cases, the frequency of the A species was determined by adding half the calculated splitting derived from the internal rotation parameters to the central frequency of the transition. Those corrected frequencies were then used in the centrifugal distortion fit. Furthermore, many transitions showed effects due to the quadrupole interaction of the ^{14}N nucleus, but a lineshape analysis was not performed due to additional complications such as internal rotation splittings and other transitions interfering with the lineshape. For such transitions no frequencies are reported.

III. Results

The assignment of the high-J Q-branch lines was strongly assisted by the characteristic doublet structure due to internal rotation splitting, which shows a smooth trend in its behaviour with J and K_a. At first sight, it is expected that one should be able to fit the rotational constants A, B, C and four centrifugal distortion constants D_J, D_{JK}, δ_J and δ_K to the transitions of the main isotopic species (Table 1), and then if that gives a standard deviation higher than the experimental error to try adding a sextic centrifugal distortion term, either h_J, h_{JK} or h_K to improve the fit. This argument is based on having only a-type Q-branch

transitions for high J, and having observed only $\Delta K_a = 0$ transitions. However, due to the asymmetry of the molecule, D_K also has a significant contribution to the transition frequencies, especially at the high J quantum numbers. Four centrifugal distortion fittings were tried, using in turn D_K, h_J, h_{JK} and h_K as the eighth variable parameter, and this yielded standard deviations of 0.03, 0.09, 0.09, and 0.09 MHz, respectively. It is therefore concluded that for this species, the five quartic centrifugal constants may be fitted and represent the spectrum more faithfully than four quartic

Table 2. The observed and calculated rotational transition frequencies (in MHz) for the symmetry species A of $^{12}CH_3{}^{78}Se^{12}C^{14}N$ in the ground vibrational state.

$J'_{K_a'K_c'}$	$J''_{K_a''K_c''}$	Observed	Calc.[a]	Obs.—Calc.	$\nu_A - \nu_E$
7_{07}	6_{06}	39841.25[b]	39841.28	−0.03	—
7_{17}	6_{16}	39184.12[b]	39184.15	−0.03	—
6_{15}	5_{14}	38622.44	38622.44	0.00	1.36
6_{25}	5_{24}	36456.40	36456.39	0.01	0.92
6_{06}	5_{05}	34617.05[b]	34617.04	0.01	—
6_{16}	5_{15}	33740.75[b]	33740.73	0.02	—
5_{14}	4_{13}	32415.29	32415.31	−0.02	1.26
5_{23}	4_{22}	31862.25	31862.26	−0.01	1.42
5_{05}	4_{04}	29296.40[b]	29296.41	−0.01	—
5_{15}	4_{14}	28243.15[b]	28243.11	0.04	—
4_{13}	3_{12}	26070.45	26070.44	−0.01	1.04
4_{04}	3_{03}	23804.58[b]	23804.51	0.07	—
4_{14}	3_{13}	22687.42[b]	22687.44	−0.02	—
3_{03}	2_{02}	18098.42[b]	18098.46	−0.04	—

[a] Calculated frequencies were obtained from Eq. (1) using the least-squares adjusted spectroscopic constants (in MHz) given in Table 13 and constraining all centrifugal distortion constants to those of $^{12}CH_3{}^{80}Se^{12}C^{14}N$ (Table 1).

[b] Internal rotation splitting unresolved. Frequencies corrected by half the calculated splitting using $^{12}CH_3{}^{80}Se^{12}C^{14}N$ ground state internal rotation parameters (Table 16).

Table 3. The observed and calculated rotational transition frequencies (in MHz) for the symmetry species A of $^{12}CH_3{}^{77}Se^{12}C^{14}N$ in the ground vibrational state.

$J'_{K_a'K_c'}$	$J''_{K_a''K_c''}$	Observed	Calc.[a]	Obs.—Calc.	$\nu_A - \nu_E$
7_{07}	6_{06}	39910.06[b]	39910.03	0.03	—
7_{17}	6_{16}	39249.29[b]	39249.31	−0.02	—
6_{06}	5_{05}	34676.21[b]	34676.22	−0.01	—
6_{16}	5_{15}	33796.38[b]	33796.37	0.01	—
5_{05}	4_{04}	29345.41[b]	29345.46	−0.05	—
5_{15}	4_{14}	28289.27[b]	28289.25	0.02	—
4_{04}	3_{03}	23843.17[b]	23843.13	0.04	—
4_{14}	3_{13}	22724.12[b]	22724.13	−0.01	—

[a] See Table 2. — [b] See Table 2.

Table 4. The observed and calculated rotational transition frequencies (in MHz) for the symmetry species A of $^{12}CH_3{}^{76}Se^{12}C^{14}N$ in the ground vibrational state.

$J'_{K_a'K_c'}$	$J''_{K_a''K_c''}$	Observed	Calc.[a]	Obs.—Calc.	$\nu_A - \nu_E$
7_{07}	6_{06}	39980.48[b]	39980.47	0.01	—
7_{17}	6_{16}	39316.16[b]	39316.16	−0.00	—
6_{25}	5_{24}	36568.99	36568.95	0.04	0.96
6_{06}	5_{05}	34736.73[b]	34736.72	0.01	—
6_{16}	5_{15}	33853.35[b]	33853.38	−0.03	—
5_{23}	4_{22}	31948.37	31948.39	−0.02	1.34
5_{05}	4_{04}	29295.42[b]	29295.42	−0.00	—
5_{15}	4_{14}	28336.49[b]	28336.47	0.02	—
4_{04}	3_{03}	23882.23[b]	23882.32	−0.09	—
4_{14}	3_{13}	22761.68[b]	22761.66	0.02	—
3_{03}	2_{02}	18155.57[b]	18155.53	0.04	—

[a] See Table 2. — [b] See Table 2.

Table 5. The observed and calculated rotational transition frequencies (in MHz) for the symmetry species A of $^{12}CH_3{}^{82}Se^{12}C^{14}N$ in the ground vibrational state.

$J'_{K_a'K_c'}$	$J''_{K_a''K_c''}$	Observed	Calc.[a]	Obs.—Calc.	$\nu_A - \nu_E$
7_{07}	6_{06}	39578.90[b]	39578.93	−0.03	—
7_{17}	6_{16}	38935.04[b]	38935.06	−0.02	—
6_{15}	5_{14}	38402.11	38402.08	0.03	1.44
6_{25}	5_{24}	36243.24	36243.23	0.01	1.61
6_{06}	5_{05}	34391.38[b]	34391.30	0 08	—
6_{16}	5_{15}	33528.12[b]	33528.10	0.02	—
5_{14}	4_{13}	32234.89	32234.93	−0.04	1.25
5_{05}	4_{04}	29109.39[b]	29109.46	−0.08	—
5_{15}	4_{14}	28066.87[b]	28066.86	0.01	—
4_{04}	3_{03}	23657.40[b]	23657.40	−0.00	—

[a] See Table 2. — [b] See Table 2.

Table 6. The observed and calculated rotational transition frequencies (in MHz) for the symmetry species A of $^{13}CH_3{}^{80}Se^{12}C^{14}N$ in the ground vibrational state.

$J'_{K_a'K_c'}$	$J''_{K_a''K_c''}$	Observed	Calc.[a]	Obs.—Calc.	$\nu_A - \nu_E$
7_{07}	6_{06}	39006.89[b]	39006.93	−0.04	—
7_{17}	6_{16}	38423.89[b]	38423.90	−0.01	—
6_{24}	5_{23}	38204.58	38204.58	0.00	1.75
6_{15}	5_{14}	38034.18	38034.20	0.02	1.31
6_{25}	5_{24}	35871.24	35871.19	0.05	0.92
6_{06}	5_{05}	33904.93[b]	33904.91	0.02	—
6_{16}	5_{15}	33098.43[b]	33098.50	−0.07	—
5_{14}	4_{13}	31953.63	31953.65	−0.02	1.21
5_{23}	4_{22}	31503.86	31503.91	−0.05	1.34
5_{05}	4_{04}	28719.86[b]	28719.87	−0.01	—
5_{15}	4_{14}	27717.21[b]	27717.19	0.02	—
4_{13}	3_{12}	25717.65	25717.67	−0.02	1.03
4_{23}	3_{22}	24099.50	24099.40	−0.11	—
4_{04}	3_{03}	23368.05[b]	23368.01	0.04	—
4_{14}	3_{13}	22274.63[b]	22274.58	0.05	—
3_{03}	2_{02}	17792.86[b]	17792.86	0.01	—
3_{13}	2_{12}	16771.12[b]	16771.15	−0.04	—

[a] See Table 2. — [b] See Table 2.

terms and any one sextic term. The Hamiltonian used was

$$\begin{aligned} H_r = & \tfrac{1}{2}(B+C)\,P^2 + [A - \tfrac{1}{2}(B+C)]\,P_a^2 \\ & + \tfrac{1}{2}(B-C)\,(P_b^2 - P_c^2) \\ & - D_J\,P^4 - D_{JK}\,P^2\,P_a^2 - D_K\,P_a^4 \\ & - 2\,\delta_J\,P^2(P_b^2 - P_c^2) \\ & - \delta_K\,[P_a^2(P_b^2 - P_c^2) \\ & + (P_b^2 - P_c^2)\,P_a^2] \end{aligned} \qquad (1)$$

and the fit is shown in Table 1.

For other isotopic species and excited states, the centrifugal distortion parameters were con-

Table 7. The observed and calculated rotational transition frequencies (in MHz) for the symmetry species A of $^{13}CH_3{}^{78}Se^{12}C^{14}N$ in the ground vibrational state.

$J'_{K'_aK'_c}$	$J''_{K''_aK''_c}$	Observed	Calc.[a]	Obs.—Calc.	$\nu_A - \nu_E$
7_{07}	6_{06}	39137.12[b]	39137.15	−0.03	—
7_{17}	6_{16}	38546.66[b]	38546.65	0.01	—
6_{15}	5_{14}	38410.74	38140.77	−0.03	1.40
6_{25}	5_{24}	35974.36	35974.28	0.08	1.36
6_{06}	5_{05}	34017.03[b]	34017.03	−0.00	—
6_{16}	5_{15}	33203.07[b]	33203.07	0.00	—
5_{14}	4_{13}	32040.04	32040.04	0.00	1.69
5_{05}	4_{04}	28812.54[b]	28812.49	0.05	—
5_{15}	4_{14}	27803.68[b]	27803.65	0.03	—
4_{23}	3_{22}	24166.67	24166.73	−0.06	—
4_{04}	3_{03}	23440.38[b]	23440.38	0.00	—
4_{14}	3_{13}	22343.06[b]	22343.14	−0.08	—

[a] See Table 2. — [b] See Table 2.

Table 8. The observed and calculated rotational transition frequencies (in MHz) for the symmetry species A of $^{12}CH_3{}^{80}Se^{12}C^{14}N$ in the first excited torsional state.

$J'_{K'_aK'_c}$	$J''_{K''_aK''_c}$	Observed	Calc.[a]	Obs.—Calc.	$\nu_A - \nu_E$
7_{07}	6_{06}	39663.33	39663.29	0.04	−12.48
7_{17}	6_{16}	39015.51	39015.55	−0.04	−12.72
6_{24}	5_{23}	38444.46	38444.37	0.09	−39.65
6_{15}	5_{14}	38430.96	38430.90	0.06	−37.06
6_{25}	5_{24}	36286.22	36286.18	0.04	−64.58
6_{06}	5_{05}	34460.11	34460.06	0.05	−13.97
6_{16}	5_{15}	33595.02	33595.06	−0.04	−12.66
5_{14}	4_{13}	32254.43	32254.48	−0.05	−35.23
5_{23}	4_{22}	31710.72	31710.71	0.01	+12.19
5_{24}	4_{23}	30352.87	30352.81	0.06	−101.35
5_{05}	4_{04}	29161.89	29161.87	0.02	−14.79
4_{13}	3_{12}	25940.91	25941.02	−0.11	−12.54
5_{15}	4_{14}	28120.81	28120.84	−0.03	−32.45
4_{04}	3_{03}	23694.22	23694.22	−0.00	−13.55
4_{14}	3_{13}	22588.96	22589.00	−0.04	−12.84
3_{12}	2_{11}	19529.75	19529.90	−0.15	−24.54
3_{03}	2_{02}	18014.07	18014.16	−0.09	−10.19

[a] See Table 2. — [b] See Table 2.

Table 9. The observed and calculated rotational transition frequencies (in MHz) for the symmetry species A of $^{12}CH_3{}^{80}Se^{12}C^{14}N$ in the $v_{10} = 1$ vibrationally excited state.

$J'_{K'_aK'_c}$	$J''_{K''_aK''_c}$	Observed	Calc.[a]	Obs.—Calc.	$\nu_A - \nu_E$
7_{07}	6_{06}	39749.72[b]	39749.75	−0.03	—
7_{17}	6_{16}	39090.85[b]	39090.81	0.04	—
6_{15}	5_{14}	38608.69	38608.89	0.00	1.89
6_{25}	5_{24}	36416.56	36416.49	0.01	1.37
6_{06}	5_{05}	34544.58	34544.61	−0.03	—
6_{16}	5_{15}	33663.39	33663.36	0.03	—
5_{14}	4_{13}	32408.81	32408.83	−0.02	1.73
5_{23}	4_{22}	31857.15	31857.19	−0.04	1.89
5_{24}	4_{23}	30464.46	30464.40	0.06	1.19
5_{05}	4_{04}	29242.91	29242.95	−0.04	0.58
5_{15}	4_{14}	28180.86[b]	28180.90	−0.04	—
4_{13}	3_{12}	26068.18	26068.20	−0.02	1.45
4_{04}	3_{03}	23768.33[b]	23768.19	0.14	—
4_{14}	3_{13}	22639.33[b]	22639.41	−0.08	—
3_{03}	2_{02}	18075.84[b]	18075.92	−0.08	—

[a] See Table 2. — [b] Internal rotation splittings unresolved. Frequencies corrected by half the calculated splitting using the internal rotation parameters for the stete $v_{10} = 1$ (Table 16).

Table 10. The observed and calculated rotational transition frequencies (in MHz) for the symmetry species A of $^{12}CH_3{}^{80}Se^{12}C^{14}N$ in the $v_{10} = 2$ vibrationally excited state.

$J'_{K'_aK'_c}$	$J''_{K''_aK''_c}$	Observed	Calc.[a]	Obs.—Calc.	$\nu_A - \nu_E$
7_{07}	6_{06}	39792.90	39792.90	0.00	0.80
6_{15}	5_{14}	38706.38	38706.35	0.03	2.92
6_{25}	5_{24}	36484.30	36484.23	0.07	2.00
5_{14}	4_{13}	32493.15	32493.16	−0.01	2.62
5_{23}	4_{22}	31932.98	31933.02	−0.04	3.15
5_{24}	4_{23}	30522.38	30522.34	0.04	1.52
5_{05}	4_{04}	29285.08	29285.16	−0.08	0.86
4_{13}	3_{12}	26137.39	26137.43	−0.04	2.22

[a] See Table 2.

Table 11. The observed and calculated rotational transition frequencies (in MHz) for the symmetry species A of $^{12}CH_3{}^{78}Se^{12}C^{14}N$ in the $v_{10} = 1$ vibrationally excited state.

$J'_{K'_aK'_c}$	$J''_{K''_aK''_c}$	Observed	Calc.[a]	Obs.—Calc.	$\nu_A - \nu_E$
7_{07}	6_{06}	39883.79[b]	39883.78	0.01	—
7_{17}	6_{16}	39217.92[b]	39217.92	−0.00	—
6_{25}	5_{24}	36525.29	36525.29	−0.00	1.29
5_{14}	4_{13}	32500.92	32500.94	−0.02	1.75
5_{23}	4_{22}	31940.73	31940.73	0.00	1.96
5_{05}	4_{04}	29338.43	29338.44	−0.01	—
5_{15}	4_{14}	28270.83[b]	28270.83	−0.00	—
4_{13}	3_{12}	26140.95	26140.92	0.03	1.50

[a] See Table 2. — [b] See Table 9.

Table 12. The observed and calculated rotational transition frequencies (in MHz) for the symmetry species A of $^{13}CH_3{}^{80}Se^{12}C^{14}N$ in the $v_{10}=1$ vibrationally excited state.

$J'_{K_a'K_c'}$	$J''_{K_a''K_c''}$	Observed	Calc.[a]	Obs.–Calc.	$\nu_A-\nu_E$
7_{07}	6_{06}	39048.27[b]	39048.27	0.00	—
7_{17}	6_{16}	38456.61[b]	38456.64	−0.03	—
6_{15}	5_{14}	38131.16	38131.14	0.02	1.90
6_{25}	5_{24}	35938.68	35938.62	0.06	1.36
6_{06}	5_{05}	33946.75[b]	33946.73	0.02	—
5_{14}	4_{13}	32037.61	32037.67	−0.06	1.69
5_{05}	4_{04}	28760.89[b]	28760.92	−0.03	—

[a] See Table 2. — [b] See Table 9.

strained to those of the ground state as fewer transitions were observed. The fits obtained for all measured CH_3SeCN species are listed in Tables 1–11 and comparison of the rotational constants and inertial defects of these species are shown in Table 12. It can be seen that the ground state inertial defects are somewhat higher than expected for a molecule with a planar heavy atom structure and a methyl group, but examination of the rotational constants and inertial defects of the $v_{10}=1$ and $v_{10}=2$ states shows a regular trend — specifically the increase of the inertial defect by about 1 uÅ^2 per excitation of v_{10}. If the inertial defects are corrected for the contribution due to v_{10}, an inertial defect of -3.343 uÅ^2 is obtained for the main species. Knowing that $v_{10}=168$ cm^{-1} from the Raman spectrum [2], we can perform a crude calculation predicting the change of inertial defect with v_{10} using

$$\Delta(v_{10}=1)-\Delta(v_{10}=0)=8\,K/\omega_{10}$$

(where $K=h/8\pi^2c=16.8627$ uÅ^2/cm) based on the formulation of Herschbach and Laurie [4], and this yields 0.80 uÅ^2, as compared with the experimental value obtained of 0.981 uÅ^2, which considering the crudity of the calculation, accounts for the magnitude of this effect.

IV. Structure

Not enough isotopic species have been measured to perform a complete structural determination, but the analysis that was done consisted of first calculating the r_s-coordinates of the selenium atom and the methyl carbon atom, using the rotational constants corrected for the zero point effect of v_{10}, and applying the appropriate Kraitchman equation [5]. This yields an r_s value for the $(H_3)C$–Se internuclear distance of 1.956 Å, and also an r_s value for the angle the $(H_3)C$–Se bond makes with the z-axis of 70.4 degrees. A least squares fitting of the v_{10}-corrected rotational constants was then performed

Table 13. Rotational constants and inertial defects of observed methyl selenocyanate species (symmetry A-species).

	A MHz	B MHz	C MHz	Inertial defect (uÅ^2)
$^{12}CH_3{}^{80}Se^{12}C^{14}N$	10143.87	3483.6892	2631.6454	− 2.8523
$^{12}CH_3{}^{80}Se^{12}C^{14}N$ ($v_{10}=1$)	10245.53 (26)	3495.7129 (49)	2631.8711 (49)	− 1.8704
$^{12}CH_3{}^{80}Se^{12}C^{14}N$ ($v_{10}=2$)	10353.82 (36)	3507.5426 (73)	2632.0672 (73)	− 0.8863
$^{12}CH_3{}^{80}Se^{12}C^{14}N$ ($v_\tau=1$) A state	10096.61 (26)	3474.4203 (51)	2629.9600 (51)	− 3.3491
$^{12}CH_3{}^{78}Se^{12}C^{14}N$	10197.88 (13)	3492.6571 (25)	2640.4335 (25)	− 2.8544
$^{12}CH_3{}^{78}Se^{12}C^{14}N$ ($v_{10}=1$)	10300.42 (89)	3504.7249 (17)	2640.6594 (17)	− 1.8704
$^{12}CH_3{}^{77}Se^{12}C^{14}N$	10226.57 (20)	3497.3435 (142)	2644.9260 (142)	− 2.8474
$^{12}CH_3{}^{76}Se^{12}C^{14}N$	10254.50 (23)	3501.9120 (57)	2649.5829 (57)	− 2.8596
$^{12}CH_3{}^{82}Se^{12}C^{14}N$	10092.31 (26)	3475.0080 (47)	2623.1991 (47)	− 2.8345
$^{13}CH_3{}^{80}Se^{12}C^{14}N$	9725.64 (16)	3454.9518 (34)	2586.4540 (34)	− 2.8455
$^{13}CH_3{}^{80}Se^{12}C^{14}N$ ($v_{10}=1$)	9826.70 (31)	3466.8065 (54)	2586.6358 (54)	− 1.8250
$^{13}CH_3{}^{78}Se^{12}C^{14}N$	9781.08 (23)	3463.1436 (45)	2594.9701 (45)	− 2.8466

Table 14. Structural Parameters of CH_3SeCN.

$r((H_3)C-Se)$ [Å]	1.956[a]
$r(Se-C(N))$ [Å]	1.837[c]
$r(C\equiv N)$ [Å]	1.170[b]
$r(C-H)$ [Å]	1.08[b]
$\angle(H-C-Se)$ [°]	107.0[b]
$\angle(C-Se-C)$ [°]	96.1[c]

[a] Determined from the r_s coordinate analysis.

[b] Constrained values. The C≡N distance was constrained to that of the r_s value in CH_3SCN, and the methyl geometry derived from the mean of the in-plane and out-of-plane methyl hydrogen r_s structural parameters in CH_3SCN [6].

[c] Determined using an r_0 structure fitting to the v_{10}-corrected rotational constants, constraining all other structural parameters.

constraining the $(H_3)C$–Se distance to the value obtained from the r_s coordinates, and also constraining the methyl group geometry and C≡N distance. The C≡N internculear distance was constrained to 1.170 Å, which is the value derived from the r_s-structure of CH_3SCN [6]. The methyl group parameters assumed were 1.080 Å for the C–H distance and 107 degrees for the H–C–Se angle. These numbers are essentially the mean of the r_s values for the in-plane and for the out-of-plane methyl group parameters in CH_3SCN. Finally the Se–C–N chain was assumed to be linear and the heavy atom structure assumed to be planar. The Se–C(N) distance and the C–Se–C bond angle were then fitted and the structural parameters are given in Table 14. It should be appreciated that the derived structure is essentially an r_0 structure, except that corrections have been applied to account for the disproportionately large contributions of the zero-point effects of v_{10} to the moments of inertia, and that certain constraints have been applied derived from an incomplete r_s analysis and by analogy with the molecule CH_3SCN. It can be seen that the Se–C(N) distance is about 0.14 Å shorter than that of H_3C–Se. The r_s structure of CH_3SCN [6] shows that the S–C(N) distance is also about 0.14 Å shorter than that of H_3C–S, and it can be concluded on this basis that the selenium atom and the sulphur atom form similar X–C bonds in these molecules.

V. Internal Rotation

The presence of a methyl group in the molecule gives rise to internal rotation, and indeed some of the ground-state lines were observed to be split. These splittings were fitted to a PAM Hamiltonian [7] assuming only the three-fold term in the potential $V(\tau)=\frac{1}{2}V_3(1-\cos 3\tau)$, and including contributions up to 4th order.

In the first excited torsional state, the magnitude of the splittings is far greater than in the ground torsional state. For the transitions in the first excited torsional state ($v_\tau=1$), the methyl group moment of inertia I_α was constrained, and both the barrier height V_3 and the angle of the methyl group with z-axis were fitted. The results of the fitting in the first excited torsional state are shown in Table 15. The difference between the θ_z obtained from this fit and the angle between the $(H_3)C$–Se bond and z-axis calculated from the r_s-coordinates suggests that the tilting of the methyl group is of the order of 1.5 degrees. For transitions arising from the ground torsional state, the results were somewhat insensitive to the value of θ_z, so it was constrained to 69°. (This is very close to the θ_z obtained from the fit in the excited torsional state, and also from the angle between the $(H_3)C$–Se bond and z-axis calculated from the r_s-coordinates.) The splitting of transitions for any rotational level increases with excitation of v_{10}, suggesting that the effective barrier height decreases strongly as a function of v_{10}. This behaviour of barrier height

Table 15. Internal rotation splittings in $^{12}CH_3{}^{80}Se^{12}C^{14}N$ in the first excited torsional state.

$J'_{K'_aK'_c}$	$J''_{K''_aK''_c}$	Observed splitting	Calculated splitting	Obs.—calc.
3_{03}	2_{02}	− 10.19	− 10.17	− 0.02
3_{12}	2_{11}	− 24.54	− 24.19	− 0.35
4_{14}	3_{13}	− 12.84	− 12.96	0.12
4_{04}	3_{03}	− 13.55	− 13.59	− 0.04
4_{13}	3_{12}	− 32.45	− 32.27	− 0.18
5_{15}	4_{14}	− 12.54	− 12.70	0.17
5_{05}	4_{04}	− 14.79	− 14.82	− 0.03
5_{24}	4_{23}	−101.35	−101.51	0.16
5_{23}	4_{22}	+ 12.99	+ 13.53	− 0.54
5_{14}	4_{13}	− 35.23	− 35.08	− 0.16
6_{16}	5_{15}	− 12.66	− 12.89	0.23
6_{06}	5_{05}	− 13.97	− 14.07	0.10
6_{25}	5_{24}	− 64.58	− 64.70	0.13
6_{15}	5_{14}	− 37.06	− 36.93	− 0.13
6_{24}	5_{23}	− 39.65	− 40.08	0.43
7_{17}	6_{16}	− 12.72	− 12.96	0.24
7_{07}	6_{06}	− 12.48	− 12.63	0.15

$I_\alpha = 3.212$ uÅ² (constrained);
$\theta_z = 68.70°$ (4), $F = 161.8$ GHz;
$V_3 = 1258.2(5)$ Cal/mol $= 5264.3(21)$ J/mol, $s = 36.23$.

Table 16. Internal rotation splittings of $^{12}CH_3{}^{80}Se^{12}C^{14}N$ in the ground torsional state, for $v_{10} = 0$, 1 and 2.

$J'_{K_a'K_c'}$	$J''_{K_a''K_c''}$	Observed splitting	Calculated splitting	Obs.—calc.
$v_{10} = 0$				
3_{12}	2_{11}	0.93	0.87	0.06
4_{13}	3_{12}	1.09	1.11	− 0.02
5_{23}	4_{22}	1.46	1.52	− 0.05
5_{24}	4_{23}	0.83	0.83	− 0.00
5_{14}	4_{13}	1.24	1.30	0.06
6_{25}	5_{24}	0.96	0.99	− 0.03
6_{15}	5_{14}	1.41	1.42	− 0.01
6_{24}	5_{23}	1.79	1.84	− 0.05
8_{17}	8_{18}	5.98	5.97	0.01
9_{18}	9_{19}	6.82	6.83	0.01
10_{28}	10_{29}	6.68	6.75	− 0.07
$v_{10} = 1$				
4_{13}	3_{12}	1.45	1.46	− 0.01
5_{05}	4_{04}	0.58	0.56	0.02
5_{24}	4_{23}	1.19	1.07	0.12
5_{23}	4_{22}	1.89	2.01	− 0.12
5_{14}	4_{13}	1.73	1.71	0.02
6_{25}	5_{24}	1.37	1.30	0.07
6_{15}	5_{14}	1.89	1.87	0.02
$v_{10} = 2$				
4_{13}	3_{12}	2.19	2.22	− 0.03
5_{05}	4_{04}	0.96	0.86	0.10
5_{24}	4_{23}	1.62	1.53	0.09
5_{23}	4_{22}	2.94	3.15	− 0.21
5_{14}	4_{13}	2.68	2.61	0.07
6_{25}	5_{24}	2.00	1.94	0.06
6_{15}	5_{14}	2.92	2.86	0.06
7_{07}	6_{06}	0.80	0.60	0.20

$I_\alpha = 3.212$ uÅ^2 (constrained);
$\theta_z = 69°$ (constrained), F = 161.8 GHz;
V_3 ($v_{10} = 0$) = 1243.7(10) Cal/mol = 5203.6(4) J/mol, $s = 35.83$;
V_3 ($v_{10} = 1$) = 1178.5(42) Cal/mol = 4930.8(18) J/mol, $s = 33.93$;
V_3 ($v_{10} = 2$) = 1082.1(44) Cal/mol = 4527.5(18) J/mol, $s = 31.17$.

with v_{10} is analogous to that of CH_3SCN [8]. However, only effective v_3 values are reported, and a full torsion-vibration-rotation treatment similar to that of Andresen and Dreizler [9] has not been attempted. The results of the fitting in the ground torsional state, and in the $v_{10} = 0$, 1 and 2 vibrational states are shown in Table 16.

The close fit of the transitions in the $v_{10} = 1$ and $v_{10} = 2$ vibrational states to an asymmetric rotor Hamiltonian and the very regular increase of the rotational constants and inertial defect with v_{10} discussed earlier, coupled with the fairly regular increase of effective barrier height with v_{10} and the similarity of the effective barrier heights between molecules in the ground and first torsionally excited states suggest very strongly that Coriolis coupling between the C–Se–C bending mode and torsional mode is very weak. A similar assertion has been made for CH_3SCN [10], but with less data.

Table 17 shows comparison of some CH_3X-bonded molecules for X being O, S and Se. There is always a decrease in barrier height on going from the sulphur to the selenium species, but the behaviour with respect to oxygen and sulphur species is irregular. It is however felt that $(CH_3)_2X$ molecules are not representative of these molecules due to extra interactions between the bulky methyl groups, especially for the small C–O distance, and that CH_3OCN would have a barrier to internal rotation of somewhat lower than 1570 cal/mole.

VI. Dipole Moments

The Stark shifts of the M-components of the $4_{04} \leftarrow 3_{03}$ and $4_{14} \leftarrow 3_{13}$ transitions were measured as a function of applied electric field, and the dipole moment components were fitted. The cell was first calibrated using OCS.

μ_a was found to be 4.18 ± 0.05 D, and μ_b to be 0.74 ± 0.03 D, where the errors are one standard deviation. It is because of this lower value of μ_b that b-type transitions were unable to be found. The total dipole moment $\mu_{tot} = 4.24 \pm 0.05$ D is comparable to the liquid-phase dipole moment [3] $\mu_b = 0.39$ D and a total dipole moment $\mu_{tot} = 4.13$ D. These numbers are very close to those of CH_3SCN [6], which has been measured to give $\mu_a = 4.11$ D.

Furthermore, the relative signs of μ_a and μ_b have been determined for CH_3SCN [10]. It has been shown from arguments based on a quadrupole

Table 17. Comparison of internal rotation barriers (in Cal/mol) for some CH_3X-Y molecules where X is O, S or Se.

	X = O	X = S	X = Se
CH_3-X-CN	—	1570[a]	1244
CH_3-X-H	1072[b]	1270[c]	1000[d]
CH_3-X-CH_3	2560[e]	2130[f]	1500[g]

[a] from Ref. [8],
[b] from Ref. [12],
[c] from Ref. [13],
[d] from Ref. [14],
[e] from Ref. [15],
[f] from Ref. [16],
[g] from Ref. [17].

analysis [11] that in CH_3SCN, there is approximately a 10% contribution of the structure CH_3–^+S=C=N^- to the bonding, and it is felt that a similar amount of the corresponding ionic resonance structure contributes to the bonding in CH_3SeCN. This conclusion is based on the similar difference between the H_3C–X and X–CN distances and also on the similar total dipole moments of the two molecules *.

**Note added in proof.* It has come to my attention that similar work has been done on CH_3SeCN by Sakaizumi et al. and their results are in essential agreement with those reported in this paper.

Acknowledgements

The author wishes to thank Dr. Manfred Winnewisser for commenting on the manuscript. The work was supported in part by the Deutsche-Forschungsgemeinschaft and the Fonds der Chemischen Industrie through the grants of Dr. Manfred Winnewisser. The Hewlett-Packard MRR spectrometer was made available through the grants of Dr. Gisbert Winnewisser by the Max Planck-Institut für Radioastronomie in Bonn. The author is also very grateful to the Alexander von Humboldt-Stiftung for the award of a Research Fellowship.

[1] E. E. Aynsley, N. N. Greenwood, and M. J. Sprague, J. Chem. Soc. 2395, (1965).
[2] W. J. Franklin, R. L. Werner, and R. A. Ashby, Spectrochem. Acta **30a**, 387 (1974).
[3] S. Millefiori and A. Foffani, Tetrahedron **22**, 803 (1966).
[4] D. R. Herschbach and V. W. Laurie, J. Chem. Phys. **40**, 3142 (1964).
[5] J. Kraitchman, Am. J. Phys. **21**, Eq. (25) (1953).
[6] H. Dreizler, H. D. Rudolph, and H. Schleser, Z. Naturforsch. **25a**, 1643 (1970).
[7] D. R. Herschbach, J. Chem. Phys. **31**, 91, Eq. (6) (1959).
[8] H. Dreizler and A. M. Mirri, Z. Naturforsch. **23a**, 1313 (1968).
[9] U. Andresen and H. Dreizler, Z. Naturforsch. **29a**, 797 (1976).
[10] S. Nakagawa, S. Takahashi, T. Kojima, and C. C. Lin, J. Chem. Phys. **43**, 3583 (1965).
[11] R. G. Lett and W. H. Flygare, J. Chem. Phys. **47**, 4730 (1967).
[12] R. M. Lees and J. G. Baker, J. Chem. Phys. **48**, 5299 (1968).
[13] T. Kojima and T. Nishikawa, J. Phys. Soc. Japan **12**, 680 (1957).
[14] C. H. Thomas, J. Chem. Phys. **59**, 70 (1973).
[15] H. Lutz and H. Dreizler, Z. Naturforsch. **30a**, 1782 (1975).
[16] L. Pierce and M. Hayashi, J. Chem. Phys. **35**, 479 (1961).
[17] J. F. Beecher, J. Mol. Spectr. **21**, 414 (1966).